films and from their dispersion on the surface of TiO_2, a catalyst known to be thermally and photochemically reactive with adsorbed, oxidizable organic substrates.[5] The larger fractional weight loss associated with the thermal decomposition of the polymers in this composite indicates that the decomposition pathway proposed for anodic PPyTs and $PPyClO_4$ (loss of anions and nitrogen to form residual activated carbon films) does not apply to the photoelectrochemically generated films, where further decomposition of the carbonaceous film proceeds. However, the relative order of thermal stability of the photoelectrochemically generated composites mirrored that in the anodic films, with $PPyBF_4$ being more stable than PPyTs.

Conclusions

The conductivity, morphology, and thermal stability of electrochemically generated polypyrrole films were predictable, reproducible, and dependent on the electrolyte in the presence of which they were produced. Although these properties could be altered by either the cation or anion, greater sensitivity to the dopant anion was observed. An interdependence of conductivity and morphology was clear: polypyrrole with the smoothest morphology (at 1000× magnification) had the highest conductivity. Thermal stability and conductivity were independent, although both of these properties showed some dependence on morphology.

Polypyrrole could be produced in a conducting form by photoelectrochemical deposition on TiO_2. The physical properties of resulting polymer composites differed significantly from those of the anodically grown polymers. The presence of dopant anions during the photoelectrochemical polymerization influenced the yield of polymer but not its conductivity or morphology. The polymeric film in the resulting composite was smoother, more uniform, and less thermally stable than the electrochemically generated films. Neither technique appears applicable for the synthesis of polypyrrole films that can be thermally decomposed to highly crystalline carbon fibers.

Acknowledgment. We acknowledge partial support of this work by General Dynamics Corp., by the Texas Advanced Research Program, and by the U.S. Army Research Office. We are grateful to Professor Harris Marcus for helpful discussions, to Robert Meegan for assistance in the ESR measurements, and to Walter Torres for measuring the UV-visible absorption spectra of the neutral and oxidized polypyrroles.

Registry No. TEATS, 733-44-8; $TEAClO_4$, 2567-83-1; $TEAPF_6$, 429-07-2; $TEABF_4$, 429-06-1; $TBAClO_4$, 1923-70-2; $TBAPF_6$, 3109-63-5; $TBABF_4$, 429-42-5; TiO_2, 13463-67-7; pyrrole (homopolymer), 30604-81-0.

Pyrolysis Chemistry of an Organometallic Precursor to Silicon Carbide

Wayde R. Schmidt,*,† Leonard V. Interrante,‡ Robert H. Doremus,† Todd K. Trout,‡ Paul S. Marchetti,§ and Gary E. Maciel§

Department of Materials Engineering, Rensselaer Polytechnic Institute, Troy, New York 12180-3590; Department of Chemistry, Rensselaer Polytechnic Institute, Troy, New York 12180-3590; and Department of Chemistry, Colorado State University, Fort Collins, Colorado 80523

Received July 3, 1990. Revised Manuscript Received December 6, 1990

The cross-linking reactions and decomposition of a vinylic polysilane precursor to silicon carbide were systematically investigated in the course of thermolysis to 1000 °C in N_2. The polymer-to-ceramic conversion chemistry was studied by means of thermogravimetry, infrared spectroscopy, solid-state NMR spectroscopy (^1H CRAMPS; ^{13}C and ^{29}Si magic-angle spinning), X-ray powder diffraction, and elemental analysis of isolated solid intermediates. Gaseous byproducts were analyzed by gas chromatography, mass spectrometry, and infrared spectroscopy. The polymer primarily undergoes cross-linking through the vinyl groups below 300 °C, although there is evidence for some hydrosilylation. Decomposition reactions consist of chain scission, with production of radical species, and methylene insertion, which converts the polysilane backbone to polycarbosilane. Crystallization to carbon-rich β-SiC ceramic occurs above 750 °C.

Introduction

Silicon carbide is an advanced ceramic material with high thermal and chemical stability, low density, high mechanical strength and hardness, and high thermal conductivity. SiC is also a high-temperature semiconductor. These attributes combine to make SiC attractive for use as fiber and matrix materials in advanced composites, oxidation resistant coatings, mechanical abrasives, furnace elements, and electronic components.[1-3]

Several researchers have prepared SiC-containing ceramics by the thermal decomposition of organosilicon polymeric precursors.[4-9] Such precursors offer potential

† Department of Materials Engineering, Rensselaer Polytechnic Institute.
‡ Department of Chemistry, Rensselaer Polytechnic Institute.
§ Colorado State University.

(1) Greenwood, N. N.; Earnshaw, A. *Chemistry of the Elements*; Pergamon Press: New York, 1984; p 386.
(2) Edington, J. W.; Rowcliffe, D. J.; Henshall, J. L. *Powder Metall. Int.* **1975**, *7*(2), 82.
(3) Edington, J. W.; Rowcliffe, D. J.; Henshall, J. L. *Powder Metall. Int.* **1975**, *7*(3), 136.
(4) Baker, W. O.; Grisdale, R. O.; Winslow, F. H. U.S. Patent 2,697,029, Dec 14, 1954.

0897-4756/91/2803-0257$02.50/0

processing advantages over traditional solid-state methods[1] due to their low decomposition temperature, solubility, thermoplasticity, and potential for microstructural control of the ceramic product.

Yajima and co-workers converted poly(dimethylsilanes), $-(Me_2Si)_n-$, to a partially cross-linked poly(carbosilane) having the approximate formula $-(MeSi(H)CH_2)_n-$ by heating in argon to 400 °C.[5] This poly(carbosilane) was melt-spun into fibers, oxidized in air at 350 °C, and converted to predominantly β-SiC, mixed with excess carbon and SiO_2, on heating in N_2 to 1300 °C. West et al.[6a] prepared a "poly(silastyrene)" copolymer, by Na/K reduction of mixtures of Me_2SiCl_2 and $PhMeSiCl_2$, which converted to silicon carbide after photoinduced cross-linking and thermolysis to at least 800 °C in an inert atmosphere.

Research by Schilling and co-workers[7] has shown that poly(carbosilanes), when branched at backbone Si atoms, and vinylic polysilanes can be effective silicon carbide precursors. These precursors were prepared by refluxing various chlorinated silanes in a hydrocarbon/ether solvent blend with either potassium or sodium. The sodium-derived polysilanes retained both the vinylic and hydrido functionality of the chlorinated monomers. The vinylic polysilane undergoes thermal cross-linking in an inert atmosphere due to a combination of hydrosilylation and vinyl polymerization.[7a,b,10] Major decomposition of the polymer occurs near 400 °C, and following heating to 1200 °C, a carbon-rich SiC ceramic is produced.[7a]

Others have employed this vinylic polysilane as a precursor to SiC ceramics and in sintering studies.[11-13] Lee and Hench[11] performed preliminary cross-linking studies of the polysilane, while Bishop and co-workers[12] monitored the increasing crystallinity of the resulting SiC ceramic with increasing temperature from 1000 to 2100 °C. Bishop also observed that the addition of up to 2 wt % of B_4C to the precursor-derived SiC powder enhanced the densification of the ceramic upon sintering. Solid solutions and composites of SiC and Si_3N_4 with AlN have been prepared by copyrolysis of this vinylic polysilane with organoaluminum amides.[13]

Although extensive research has been carried out on the preparation of polymeric precursors to silicon carbide, few detailed studies of the decomposition chemistry of these materials and the nature of the intermediates in the precursor-to-ceramic conversion process have been reported. Lipowitz et al. characterized Yajima's poly(carbosilane)-derived silicon carbide fibers by XRD, IR, elemental analysis, electron microscopy, and ^{29}Si MAS NMR.[14] Poupeau et al. monitored the gaseous byproducts during the pyrolysis of the same poly(carbosilane) by GC and MS as a function of temperature and extent of oxidation.[15] Popeau found the major gaseous decomposition products to be CH_4 and H_2, with minor amounts of silane, methylsilane, ethylene, and ethane. Babonneau and coworkers have recently reported detailed descriptions of the structural conversion of poly(carbosilane) and poly(titanocarbosilanes) to SiC and SiC/TiC ceramics,[16] as determined by XRD, IR, and NMR techniques. Carlsson et al.[17] have examined the effect of substituents on poly(methylsilane) backbones on the pyrolysis yield of SiC and found improved yields for polymers derived from monomers containing unsaturated substituents. Hasegawa and Okamura also examined the decomposition of Yajima's SiC precursor by IR, UV, solution NMR, thermal analysis, XRD, and gas evolution.[9] Hasegawa recently described the oxidative curing mechanisms of the poly(carbosilane) fibers and the relationship between the structure and pyrolysis process during decomposition to 1600 °C.[9c]

The main objective of the present study was to investigate thoroughly the decomposition chemistry of Schilling's sodium-derived vinylic polysilane in an inert atmosphere such as N_2, and to characterize the polymer-to-ceramic conversion with the aid of thermal analysis, FTIR, solution- and solid-state NMR, XRD, and gas analysis methods. An understanding of the conversion chemistry of this polymer precursor is necessary to successfully control its application in electronics and as fiber and matrix materials in ceramic composites.

Experimental Section

General Methods. A sodium-derived vinylic polysilane (VPS), designated as Y-12044 by the manufacturer, was purchased from Union Carbide Corp., Tarrytown, NY. The exact composition of VPS was not disclosed by Union Carbide Corp., but molar ratios of 0.85 Me_3SiCl, 0.3 Me_2SiCl_2, and/or $MeSiHCl_2$, and 1.0 $CH_2{=}CHSiMeCl_2$ are reported for the starting silanes.[7a] VPS is a translucent, viscous, liquid polymer that is known to undergo thermal cross-linking.[7a,b,10]

Nitrogen was purified in-line by deoxygenation over activated copper catalyst and dried over 3-Å molecular sieves. This purified N_2 was used for all glovebox operations, TGA experiments, and thermal decomposition reactions. Transmission infrared spectra were recorded with a Perkin-Elmer 1850 FTIR spectrophotometer

(5) (a) Yajima, S.; Hasegawa, Y.; Hayashi, J.; Iimura, M. *J. Mater. Sci.* **1978**, *13*, 2569. (b) Yajima, S.; Hayashi, J.; Omori, M. *Nature* **1976**, *261*, 683. (c) Yajima, S.; Okamura, K., Hayashi, J.; Omori, M. *J. Am. Ceram. Soc.* **1976**, *59*(7-8), 324. (d) Hasegawa, Y.; Iimura, M.; Yajima, S. *J. Mater. Sci.* **1980**, *15*, 720. (e) Yajima, S.; Hayashi, J.; Omori, M. U.S. Patent 4,100,233, July 11, 1978. (f) Yajima, S. *Philos. Trans. R. Soc. London, A* **1980**, *294*, 419. (g) Yajima, S.; Hayashi, J.; Omori, M. *Chem. Lett.* **1975**, 931. (h) Yajima, S. Silicon Carbide Fibres. In *Handbook of Composites*; Watt, W., Perov, B. V., Eds.; Elsevier Science Publishers: New York, 1985; Vol. 1, Chapter VI, p 201.

(6) (a) West, R.; David, L. D.; Djurovich, P. I.; Yu, H.; Sinclair, R. *Am. Ceram. Soc. Bull.* **1983**, *62* (8), 899. (b) West, R.; Nozue, I.; Zhang, X.-H.; Trefonas, P. *Polym. Prepr., ACS Div. Polym. Chem.* **1984**, *25*, 4. (c) West, R.; David, L. D.; Djurovich, P. I.; Stearley, K. L.; Srinavasan, K. S. V.; Yu, H. *J. Am. Chem. Soc.* **1981**, *103*, 7352. (d) Mazdiyasni, K. S.; West, R.; David, L. D. *J. Am. Ceram. Soc.* **1978**, *61*, 504.

(7) (a) Schilling, C. L., Jr. *Brit. Polym. J.* **1986**, *18*(6), 355. (b) Schilling, C. L., Jr.; Wesson, J. P.; Williams, T. C. *Am. Ceram. Soc. Bull.* **1983**, *62*(8), 912. (c) Schilling, C. L., Jr.; Williams, T. C. *Polym. Prepr., ACS Div. Polym. Chem.* **1984**, *25*(1), 1. (d) Schilling, C. L., Jr. Tech. Report No. 83-3 on ONR Contract N00014-81-C-0682, Sept 1983. (e) Schilling, C. L., Jr.; Wesson, J. P.; Williams, T. C. *J. Polym. Sci., Polym. Symp.* **1983**, *70*, 121. (f) Schilling, C. L., Jr.; Williams, T. C.; Wesson, J. P. U.S. Patent No. 4,414,403, Nov 8, 1983. (g) Schilling, C. L., Jr.; Williams, T. C. U.S. Patent No. 4,472,591, Sept 18, 1984.

(8) (a) Baney, R. H.; Gaul, J. H., Jr.; Hilty, T. K. *Organometallics* **1983**, *2*, 859. (b) Baney, R. H.; Gaul, J. H., Jr. U.S. Patent 4,310,651 1982, Dow Corning Corp.

(9) (a) Hasegawa, Y.; Okamura, K. *J. Mater. Sci.* **1983**, *18*, 3633. (b) Hasegawa, Y.; Okamura, K. *J. Mater. Sci.* **1986**, *21*, 321. (c) Hasegawa, Y. *J. Mater. Sci.* **1989**, *24*, 1177.

(10) Pawlenko, S. *Organosilicon Chemistry*; Walter de Gruyter: New York, 1986; pp 35-37.

(11) Lee, B. I.; Hench, L. L. *Mater. Res. Soc. Symp. Proc.* **1986**, *73*, 815.

(12) Bishop, B. A.; Spotz, M. S.; Rhine, W. E.; Bowen, H. K.; Fox, J. R. In *Ceramic Transactions*; Messing, G. L., Fuller, E. R., Jr., Hausner, H., Eds. The American Ceramic Society: Westerville, OH, 1988, Vol. 1, Part B, p 856.

(13) (a) Czekaj, C. L.; Hackney, M. L. J.; Hurley, W. J., Jr.; Interrante, L. V.; Sigel, G. A.; Shields, P. J.; Slack, G. A. *J. Am. Ceram. Soc.* **1990**, *73*(2), 352. (b) Interrante, L. V.; Hurley, W. J., Jr.; Schmidt, W. R.; Kwon, D.; Doremus, R. H.; Marchetti, P. S.; Maciel, G. E. Preparation of Nanocrystalline Composites by Pyrolysis of Organometallic Precursors. Presented at the Second International Ceramic Science and Technology Congress, Nov 12-15, 1990, Orlando, FL.

(14) Lipowitz, J.; Freeman, H. A.; Chen, R. T.; Prack, E. R. *Adv. Ceram. Mater.* **1987**, *2*(2), 121.

(15) Poupeau, J. J.; Abbe, D.; Jamet, J. *Mater. Sci. Res.* **1984**, *17*, 287.

(16) (a) Soraru, G. D.; Babonneau, F.; Mackenzie, J. D. *J. Mater. Sci.* **1990**, *25*, 3886. (b) Babonneau, F.; Soraru, G. D.; Mackenzie, J. D. *J. Mater. Sci.* **1990**, *25*, 3664. (c) Babonneau, F.; Livage, J.; Soraru, G. D.; Carturan, G.; Mackenzie, J. D. *New J. Chem.* **1990**, *14*, 539.

(17) Carlsson, D. J.; Cooney, J. D.; Gauthier, S.; Worsfold, D. J. *J. Am. Ceram. Soc.* **1990**, *73*(2), 237.

Table I. Heating Schedules Used during the Pyrolysis of VPS in N_2 and the Morphology of the Isolated Solids

sample	heating schedule	sample appearance
VPS	none	translucent, viscous liquid
151N	25 to 151 °C in 42 min	translucent, rubbery solid
196N	25 to 196 °C in 57 min	translucent, nonporous, white glassy solid
250N	25 to 250 °C in 1 h, 250 °C hold 10 h, furnace cool	nonporous, yellow glassy solid
400N	25 to 250 °C in 1 h, 250 °C hold 3 h, 250 to 400 °C in 1 h, 400 °C hold 10 h, furnace cool	nonporous, brownish glassy solid
650N	25 to 250 °C in 2 h, 250 °C hold 3 h, 250 to 650 °C in 3 h, 650 °C hold 10 h, furnace cool	nonporous, black glassy solid
1000N	25 to 250 °C in 2 h, 250 °C hold 3 h, 250 to 1000 °C in 6 h, 1000 °C hold 10–15 h, furnace cool	nonporous, black glassy solid

equipped with a Deltech dry air purge assembly. The FTIR was operated at 4-cm^{-1} resolution with a TGS detector. Liquid and solid IR samples were prepared in a N_2-filled glovebox as smears between KBr windows or pressed as KBr (International Crystal Laboratories) pellets, respectively. Samples were transferred from the glovebox to the spectrophotometer in N_2-filled bags to minimize exposure to air and moisture.

Elemental analyses of the preceramic and ceramic materials were performed by Leco Corp., St. Joseph, MI, and Galbraith Laboratories, Inc., Knoxville, TN. X-ray diffraction (XRD) measurements were obtained using Cu Kα radiation with a Philips PW1710 automated powder diffractometer equipped with a monochromator in the exit beam. Scanning electron microscopy was performed with either an Amray 1000-A or a JEOL JSM-840II microscope at 20 keV.

Thermogravimetric analysis (TGA) of VPS was performed in flowing N_2 (0.05–0.1 standard cubic feet/hour (scfh)) with a Perkin-Elmer 7 Series thermal analysis system. Typical heating rates were 5 and 10 °C/min over the ranges of 50–700 and 700–1200 °C, respectively. Simultaneous TGA/DTA experiments were performed in N_2 with a Netzsch STA429 thermobalance. A heating rate of 20 °C/min from 25 to 1500 °C and a N_2 flow rate of 0.15–0.21 scfh were employed.

Molecular weights were determined by gel permeation chromatography (GPC) using a Waters Chromatography 600 multisolvent delivery system coupled with a 410 differential refractometer and a 745 data module. Three Waters Ultrastyragel columns (porosity ranges of 500, 10000, and 100 Å), calibrated by using polystyrene standards, were employed in series with helium-purged, filtered toluene as the eluent at a flow rate of 0.6 mL/min. VPS solutions were prepared at 0.2% by weight in toluene and filtered through 0.45-μm filters (Gelman Sciences) prior to injection of 50-μL samples.

Gas separations for GC/FTIR experiments were performed with a Varian 3700 gas chromatograph on either an Alltech VZ-10 (6 ft, 0.085-in. i.d. 60/80 mesh range) or a Chromosorb-103 (6 ft., 0.085-in. i.d., 80/100 mesh range) packed column. The GC was interfaced to the Perkin-Elmer 1850 FTIR spectrophotometer and operated in a dual detection mode (FTIR-MCT, GC-TCD).

Electron impact mass spectra were obtained on a Hewlett-Packard 5987A GC/MS system following gas separations on a cross-linked methylsilicone capillary column (25 m, 0.25-μm i.d.).

NMR Methods. All NMR measurements were obtained at ambient temperature. ^1H, ^{13}C, and ^{29}Si solution spectra were acquired by using a Varian XL-200 NMR spectrometer with benzene-d_6 or toluene-d_8 as the solvent. Chemical shift data were referenced to tetramethylsilane (TMS) in all cases.

Solid-state ^{13}C and ^{29}Si magic-angle spinning (MAS) NMR spectra were obtained in natural abundance on a modified Nicolet NT-150 spectrometer by using single-pulse excitation and proton decoupling during data acquisition. The observe frequencies were 37.74 and 29.81 MHz for carbon and silicon, respectively. A 30° excitation pulse was employed in all cases, and either a 10-s (^{13}C) or a 15-s (^{29}Si) recycle delay was used. Spectra obtained after applying a 50-Hz line broadening to the free induction decay and Fourier transformation represent the accumulation of 2000–3000 transients. Samples were spun at a rate of 2.5–4.0 kHz in cylindrical rotors[18] machined from Delrin (^{29}Si) or Kel-F (^{13}C). Under the instrumental conditions employed, there was negligible carbon background signal from the Kel-F rotors. In the case of neat liquid polymer samples, the sample was held within a Teflon insert that was fitted into the rotor and prevented sample leakage during MAS. A broad peak at 112 ppm due to Teflon appears in the carbon spectra of these samples. All carbon and silicon chemical shift data were referenced to TMS.

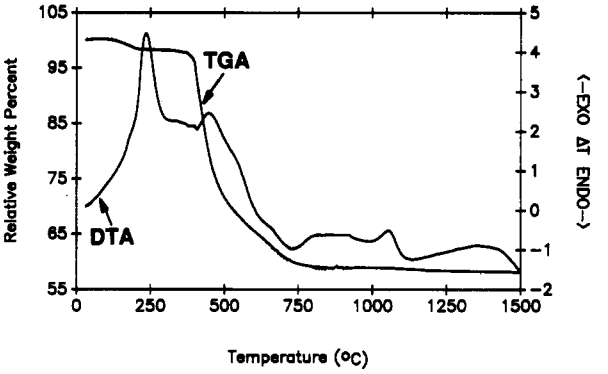

Figure 1. Thermogravimetric (TGA) and differential thermal analysis (DTA) curves for VPS heated in N_2 at a rate of 20 °C/min.

Solid-state proton NMR spectra using the CRAMPS technique were obtained on a modified Nicolet NT-187 spectrometer as described in detail by Bronnimann et al.[19] Proton chemical shifts were referenced to solid tetrakis(trimethylsilyl)methane (TTMSM) as an external standard and reported with respect to TMS. Each spectrum represents the accumulation of between 32 and 128 transients, depending on the sample proton density.

Pyrolysis of VPS. The cross-linking mechanisms of VPS were studied by slowly heating the polymer in a N_2-filled glovebox to temperatures up to 250 °C and periodically removing portions for analysis. Approximately 35 mL of VPS was placed in a Schlenk tube, under constant N_2 purge. The sample was typically heated in 1 atm of N_2 at 3 °C/h from room temperature to the first desired temperature and held for at least 1 h. Subsequently, a 2-mL portion was withdrawn for FTIR, solution- or solid-state NMR, and GPC analyses, and the remaining sample was heated to the next desired temperature. Samples were progressively heated from 22 to 250 °C in this manner.

The effect of ultraviolet light exposure on the cross-linking of VPS was also investigated by placing a portion of as-received VPS in a glass vial and irradiating it with long-wavelength UV light (UVP Model UVGL-25 lamp) for approximately 72 h under N_2.

Pyrolyzed samples were taken after heating VPS at various temperatures that followed major weight losses in the TGA curve. Pyrolysis experiments were performed by pouring weighed portions (from 5 to 20 g) of the as-received polymer into a molybdenum boat, which was then placed into a gas-tight fused silica furnace tube. All loading operations were performed in a glovebox under N_2. Polymer samples were pyrolyzed in a CM Furnaces 1000 Series programmable tube furnace according to the schedules in Table I. All pyrolyses were conducted at 1 atm under prepurified N_2 flowing at a rate of 0.3–0.5 scfh. The volatile species that evolved during heating were either analyzed in-line by GC or GC/MS or first collected in liquid N_2 (−196 °C) traps and

(18) Wind, R. A.; Anthonio, F. E.; Duijvestijn, M. J.; Smidt, J.; Trommel, J.; DeVette, G. M. C. *J. Magn. Reson.* **1983**, *52*, 424.

(19) Bronnimann, C. E.; Hawkins, B. L.; Zhang, M.; Maciel, G. E. *Anal. Chem.* **1988**, *60*, 1743.

Table II. Characteristic Infrared Absorption Bands for VPS at Room Temperature

wavenumber, cm^{-1}	assgnt	ref
3048 (m)	asym $=CH_2$ stretch	17, 21
2952 (s)	asym $-CH_3$ stretch	20–22
2894 (s)	sym $-CH_3$ stretch	20, 21
2078 (s)	Si-H stretch	17, 21, 22
1732 (w)	olefinic overtone	21
1582 (w)	C=C stretch	21, 23
1397 (s)	Si—$CH=CH_2$ deformation	20
1246 (vs)	Si—CH_3 sym deformation	20, 21, 23
1046 (s)	Si—CH_2—Si deformation	21–23
	Si—O—Si stretch	24
1004 (m), 937 (m)	Si—H bending	21, 22
750–850 (s)	Si—C stretch	17, 20–23

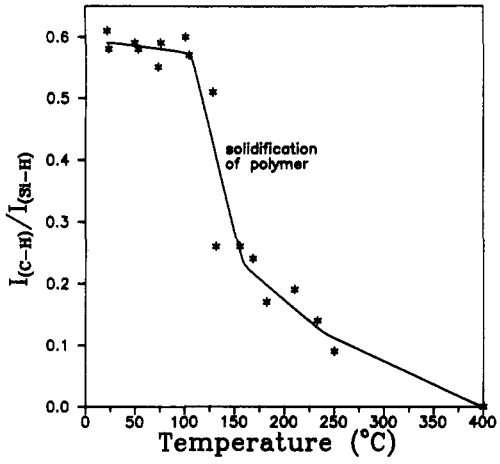

Figure 2. Relative intensities of the $C-H_{3048\ cm^{-1}}$ band and the $Si-H_{2078\ cm^{-1}}$ band in VPS as a function of temperature.

subsequently identified by GC/FTIR and GC/MS. Immediately following pyrolysis, the solid products were stored under N_2. For analysis the samples were dry-ground under N_2 to uniform fine powders in a B_4C mortar and pestle.

Results

Thermal Analysis. The TGA for VPS in N_2 is shown in Figure 1. Three main regions can be identified in the weight loss curve: (1) 50–300 °C, where the thermosetting reactions occur but relatively little weight loss is observed; (2) 300–750 °C, where extensive degradation of the polymer and major weight loss occur; (3) above 750 °C, where the weight loss is again small. The char yield for the black, glassy, solid obtained at 1000 °C is about 57%, which is consistent with Schilling's results.[7a] The associated DTA trace shows a large exotherm near 250 °C, which corresponds to the cross-linking reactions, a smaller exotherm centered near 450 °C, which is associated with the large weight loss and decomposition of the polymer, and a complicated region from 750 to 1500 °C that suggests partial crystallization of the ceramic. Schilling noted similar curves to 600 °C.[7a]

Cross-Linking of VPS. (a) Infrared spectroscopy: Infrared absorption frequencies for characteristic stretches and deformations of untreated VPS are summarized in Table II. These peak positions are comparable to literature values for polysilanes and related compounds.[17,20–24]

Table III. Effect of Increased Temperature on the Molecular Weight of VPS in N_2

temp, °C	ratio of 26000 amu/800 amu	M_w[a]	M_n[b]
22	0.16	3230	667
50	0.32	3560	821
76	0.43	15116	1040
128	0.67	20843	1331
ultraviolet	1.10	84887	1834

[a] Weight-average molecular weight. [b] Number-average molecular weight.

Table IV. Elemental Analyses (Weight Percent) for Isolated Solids Obtained during the Pyrolysis of VPS in N_2, According to Heating Schedules Outlined in Table I[25]

sample	Si	C	H	O	N	atomic Si/C	excess C
SiC (calc)	70.04	29.96	0.00	0.00	0.00	1.00	0.00
VPS as rec'd	44.73	46.31	8.88	0.60	0.09	0.41	27.2
250N	32.56	35.76	7.13	0.56	0.08	0.39	21.8
400N	39.17	37.14	7.52	0.48	0.07	0.45	20.5
650N	45.16	35.83	3.03	2.55	0.56	0.54	16.5
1000N	54.53	40.38	0.53	2.65	0.57	0.58	17.1

Atmospheric CO_2 is seen as a doublet between 2250 and 2400 cm^{-1}.

With increasing heating, the liquid VPS sample gradually increases in viscosity, becoming a semisoft, rubbery solid, with setting occurring near 140 °C; the exact temperature of solidification depends upon the heating rate. Further heating at slightly higher temperatures converts the VPS to a translucent, glassy solid. Figure 2 is a plot of the intensity of the IR absorption bands of VPS assigned to the C–H stretching mode of the pendant vinyl groups of the polysilane (3048 cm^{-1})[17,21] relative to those attributed to the Si–H stretching mode (2078 cm^{-1}),[17,21–22] as a function of temperature. Prior to the observed solidification at around 125–140 °C, the concentration of vinyl groups compared to that of Si–H groups decreases slightly upon heating. Thermosetting of the polymer is accompanied by a pronounced decrease in IR absorption at 3048 cm^{-1} relative to absorption at 2078 cm^{-1}. The slope of the curve in Figure 2 again decreases between 160 and 400 °C.

(b) Molecular weight analysis: Figure 3 displays GPC results of representative samples after heating or UV irradiation. Figure 3a is the GPC curve of as-received VPS at room temperature. As heating proceeds (Figure 3a–c) or on exposure to ultraviolet radiation (Figure 3d), the average molecular weight of the polymer increases. This trend can be quantified by comparing the amount of VPS in a high molecular weight (26 000 amu) fraction to the amount in a lower molecular weight (800 amu) fraction. Table III summarizes the increase of this ratio with increasing temperature; at 128 °C, the ratio approaches that of the UV-treated sample, confirming that the extent of cross-linking increases with temperature.

Decomposition of VPS. (a) Morphology: Isolated samples 250N, 400N, 650N, and 1000N were all smooth, nonporous glassy solids that ranged in color from yellowish to black, depending on the pyrolysis conditions (Table I). Several large chunks (1–2 cm^2) of material remained following pyrolysis. These chunks were easily broken by hand. SEM examination of the solid products showed microcracks that were typically 1 μm wide by 100 μm long; these were probably caused by expansion and contraction of the cross-linked polymer during heating and cooling. No pores were observed in the chunks by SEM, which had a

(20) Smith, A. L.; Anderson, D. R. *Appl. Spectrosc.* **1984**, *38*(6), 822.
(21) Colthup, N. B.; Daly, L. H.; Wiberley, S. E. *Introduction to Infrared and Raman Spectroscopy*; Academic Press: New York, 1964.
(22) Wu, H.-J.; Interrante, L. V. *Chem. Mater.* **1989**, *1*, 564.
(23) Bullot, J.; Schmidt, M. P. *Phys. Status Solidi B* **1987**, *143*, 345.
(24) Mutsuddy, B. *Ceram. Int.* **1987**, *13*, 41.

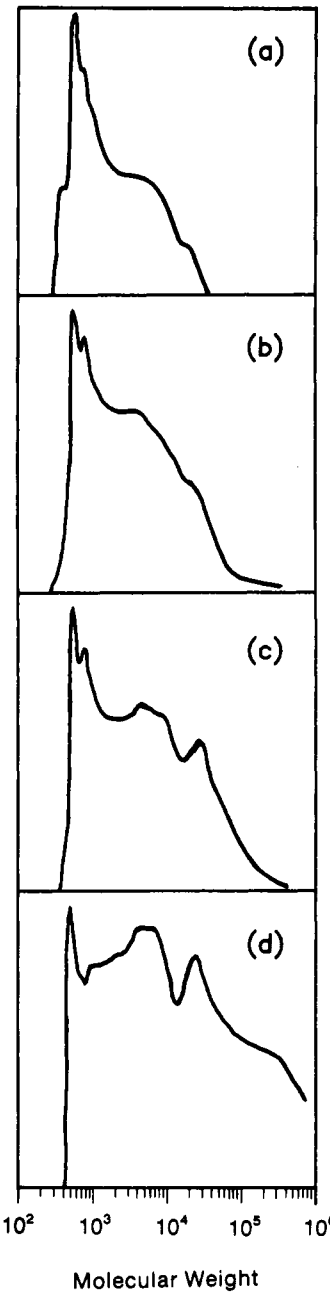

Figure 3. Gel permeation chromatograms of thermally cross-linked and UV-irradiated VPS samples: (a) 22 °C, (b) 76 °C, (c) 128 °C, (d) UV-irradiated.

resolution of 250 nm at the highest magnification used (10 000×).

(b) Elemental analysis: The elemental analyses of the preceramic samples are shown in Table IV.[25] The measured Si/C ratio increases with temperature but is significantly less than the expected unit ratio for SiC, indicating the presence of excess carbon. If all of the Si in the preceramics exists as SiC, the amount of excess carbon decreases with increasing temperature from 27.2% by weight in the as-received polymer, to 17.1% by weight in the 1000N sample. These values are consistent with those

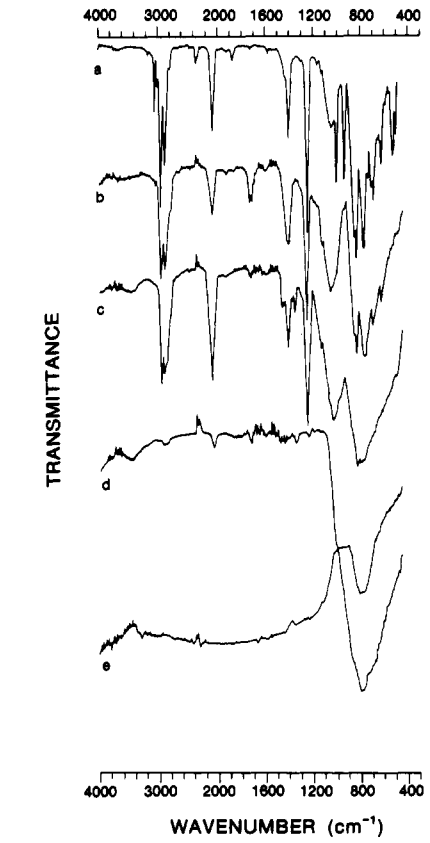

Figure 4. Transmission infrared spectra of isolated VPS samples heated according to schedules in Table I: (a) VPS, (b) 250N, (c) 400N, (d) 650N, (e) 1000N.

previously reported for the pyrolysis of VPS in N_2.[7a,12]

(c) Infrared spectroscopy: The conversion from polymeric VPS to ceramic was monitored by the changes in the transmission infrared spectra of the solid samples with increased pyrolysis temperature (Figure 4). On heating VPS from 25 to 250 °C (sample 250N), there is a decrease in the intensity of the asymmetric $=CH_2$ stretch (3048 cm^{-1}), a broadening of the $SiCH=CH_2$ deformation band (1397 cm^{-1}), and a slight decrease in both the intensity and area as well as a broadening of the Si–H band (2078 cm^{-1}). A band attributed to $Si-CH_2-Si$ deformation[21-23] occurs at 1046 cm^{-1} in the as-received sample. Mutsuddy has reported a similar band in poly(carbosilanes) to be caused by Si–O–Si deformations.[24] The band at 1046 cm^{-1} increases significantly in intensity with increased pyrolysis temperature to 650 °C (sample 650N). The intensity of the Si–H peak also increases as the pyrolysis temperature is increased from 250 to 400 °C (sample 400N), as previously noted by Schilling.[7a]

The IR spectrum of sample 650N indicates that most of the C–H and Si–H functionalities of the polymer are lost on heating to 650 °C; by 1000 °C (sample 1000N) those IR peaks that are characteristic of these groups (3200–2800 and 2078 cm^{-1}, respectively) are completely absent. The presence of a strong band centered near 800 cm^{-1}, characteristic of the Si–C stretch, in the IR spectrum of 1000N provides further evidence for the formation of ceramic SiC.[26]

(d) NMR spectroscopy: The pyrolytic conversion of VPS to ceramic SiC was investigated by observing changes in the solution- and solid-state ^1H, ^{13}C, and ^{29}Si NMR spectra as a function of temperature. The ^1H solution

(25) We have previously obtained poor results for elemental analyses of isolated intermediate solids. Analyses totalling less than 100% are probably due to low values for Si analysis. Similar low values for Si have been reported for carbosilanes and have been attributed to incomplete combustion of the compound. These observations are not considered to significantly alter the Si/C ratios obtained in this work. For more detail, see, for example, refs 6a and 28 and: Bacque, E.; Pillot, J.; Birot, M.; Dunogues, J. *Macromolecules* **1988**, *21*, 30,34.

(26) Ramis, G.; Quintard, P.; Cauchetier, M.; Busca, G.; Lorenzelli, V. *J. Am. Ceram. Soc.* **1989**, *72*(9), 1692–1697.

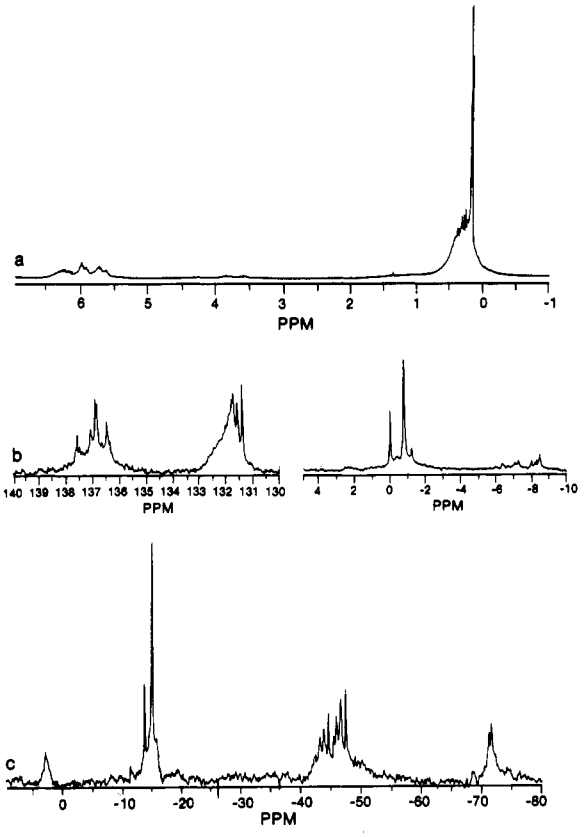

Figure 5. Solution NMR spectra of as-received VPS: (a) ^{1}H, (b) ^{13}C, (c) ^{29}Si. Peak assignments are noted in the text.

NMR spectrum of as-received VPS (Figure 5a) exhibits three major proton resonances associated with the vinyl protons[27,28] (multiplet, 5.4–6.5 ppm), hydride protons[5h,29] (two small, broad peaks, 3.6 and 3.85 ppm), and methyl and methylene protons[5h,27,28,30] (broad, complex multiplet, –0.20 to 1.0 ppm) with integrated areas (≡SiCH=CH_2:≡SiH:=$SiCH_3$ + ≡$SiCH_2$–) of ca. 5.3:1:20, respectively. The ^{1}H and ^{13}C solution NMR spectra of VPS samples heated below 150 °C (not shown) show the loss of vinyl and SiH groups as cross-linking proceeds.

The ^{1}H CRAMPS spectra of the isolated solids are shown in Figure 6. The spectra of samples 151N and 196N exhibit a small, broad peak near 6 ppm, indicative of vinyl protons. This peak decreases in intensity as the pyrolysis temperature is changed from 151 to 250 °C, where it is virtually absent. Methyl protons exhibit a sharp peak near 0 ppm. Methylene proton peaks at 1.3 and 1.1 ppm are resolved in the spectrum of 250N, suggesting the existence of more than one type of methylene environment. The peaks at 1.3 and 1.1 ppm increase in relative intensity and broaden with increased pyrolysis temperature up to 1000 °C. The position and width of the methyl proton peak near 0 ppm remain relatively constant to 400 °C. The spectra of samples 650N and 1000N show residual C–H proton resonance (centered near 0–1 ppm), which supports the infrared data. The spectra of 650N and 1000N show a lower signal-to-noise (S/N) ratio than samples 151N to

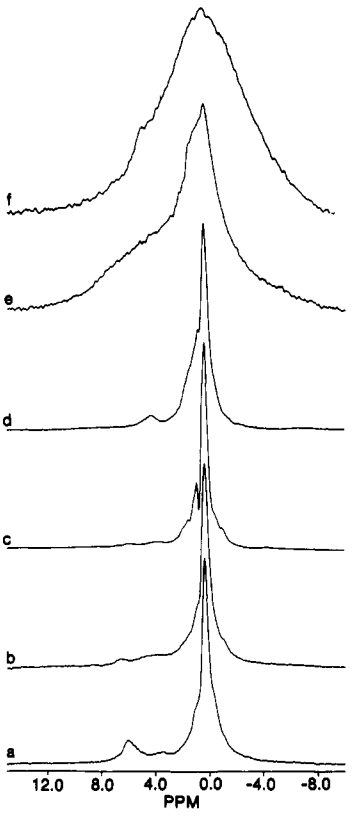

Figure 6. The 187-MHz ^{1}H CRAMPS spectra of isolated VPS samples heated according to schedules in Table I: (a) 151N, (b) 196N, (c) 250N, (d) 400N, (e) 650N, (f) 1000N. All spectra are plotted to the same vertical scale. The sample size for 650N and 1000N was about 5 times greater than the other samples, so that spectra e and f represent low levels of hydrogen (see Table IV).

400N because of the lower concentration of hydrogen in the higher temperature samples (Table IV). Only qualitative intensity comparisons can be made between spectra in Figure 6, since sample sizes were not equivalent.

A small peak indicating Si–H functionality[29] is observed near 3.5 ppm in the spectrum of 151N. This peak broadens somewhat, yet remains nearly constant in intensity, relative to the methyl/methylene resonances, with increasing temperature to 250 °C. The intensity of this peak increases in sample 400N, indicating an increased concentration of Si–H functionality, and shifts to 4–4.4 ppm. This peak is still present in the spectrum of 650N yet decreases in intensity relative to the C–H peak. The breadth of this low-shielding peak in the spectrum of 650N may be caused by overlapping C–H intensity from the graphitic phase in 650N or by physisorbed water. This peak is largely absent in the 1000N CRAMPS spectrum.

The ^{13}C solution NMR spectrum of the original VPS sample (Figure 5b) exhibits peaks indicative of $R_3Si{*}CH{=}{*}CH_2$ groups (130.5–133 and 135.5–138.5 ppm),[28] $RSi{*}Me_3$ end groups (1 to –2 ppm),[28,31,32] a mixture of $R_2Si(H){*}Me$, $R_2Si(CH{=}CH_2){*}Me$, and $R_3SiSi({*}Me_2)$-SiR_3 groups (–5 to –10 ppm),[28,32] and a minor peak attributed to a $R_3Si{*}CH_2SiR_3$ functionality (1.6–3 ppm).[28] The corresponding ^{13}C MAS spectra of as-received VPS and the isolated preceramic samples are shown in Figure 7. The ^{13}C MAS spectrum of VPS is consistent with the solution NMR results and exhibits peaks attributed to vinyl (131.9, 137.0 ppm) and end-group methyl (–0.30 ppm)

(27) Aikens, D. A.; Bailey, R. A.; Giachino, G. G.; Moore, J. A.; Tomkins, R. P. T. *Integrated Experimental Chemistry, Principles and Techniques*; Allyn & Bacon: Boston, 1978; Vol. 1, p 337.
(28) (a) Williams, E. A. In *The Chemistry of Organic Silicon Compounds*; Patai, S., Rappoport, Z., Eds.; Wiley: New York, 1989; Chapter 6. (b) Williams, E. A. In *Annual Reports on NMR Spectroscopy*; Academic Press: London, 1983; Vol. 15.
(29) Fritz, G.; Schmid, K.-H. *Z. Anorg. Allg. Chem.* **1978**, *441*, 125.
(30) Fritz, G.; Wartanessian, S. *J. Organomet. Chem.* **1979**, *178*, 11.
(31) Bacque, E.; Pillot, J.-P., Birot, M.; Dunogues, J. *J. Organomet. Chem.* **1988**, *346*, 147.
(32) Stanislawski, D. A.; West, R. *J. Organomet. Chem.* **1981**, *204*, 295.

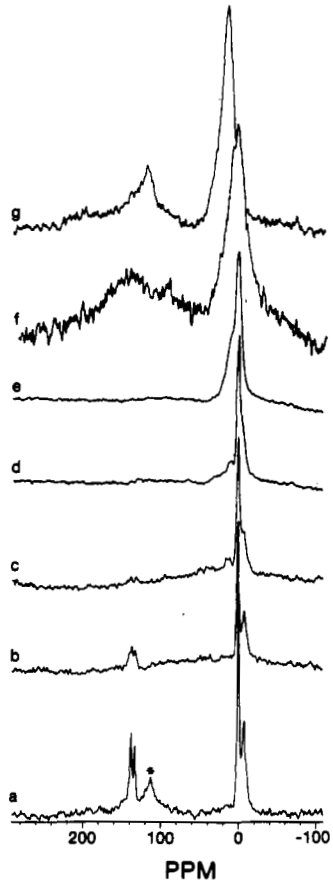

Figure 7. The 37.74-MHz ^{13}C MAS NMR spectra of isolated VPS samples heated according to schedules in Table I: (a) VPS, (b) 151N, (c) 196N, (d) 250N, (e) 400N, (f) 650N, (g) 1000N. The artifact peak at 112 ppm from the Teflon rotor insert is noted in (a) with an asterisk.

functionality, as well as a high-shielding peak at −6.95 ppm, representing the methyl functionality of H- and/or vinyl-substituted silicon and dimethylsilane units. A small peak at 10 ppm is attributed to the minor carbosilane fraction. The ^{13}C MAS NMR spectrum of the rubbery solid isolated at 151 °C is very similar to that of neat VPS, except for a decrease in the vinyl resonance intensity; sharp peaks at 0.30 ppm (*Me_3Si end groups) and −6.95 ppm (*MeSiH, *MeSi–vinyl, and *Me_2Si units) are also seen. After pyrolysis at 196 °C, the intensities of peaks associated with the vinyl groups decrease significantly relative to those from the methyl/methylene groups, as compared to the sample obtained at 151 °C. There is increased intensity of a small peak at 11.5 ppm, which is attributed to an ethylene bridge between silicon atoms. A second methylene resonance is barely discernible near 30 ppm. The peak originally at −6.95 ppm in VPS is shifted to lower shielding (−5.8 ppm) in the 196N sample. By 250 °C the peaks originally at 137.0 and 131.9 ppm in VPS are nearly gone, indicating that reactions at vinyl groups are complete at this stage of thermolysis. The large peak at 0.30 ppm in VPS is shifted to a slightly more shielded −0.31 ppm in 250N. The position of the peak at 11.5 ppm remains unchanged by pyrolysis at 250 °C, but increased peak intensity indicative of new methylene functionality is seen near 8.3 and 30 ppm. In sample 400N, the shoulder at −5.8 ppm and the peak at −0.31 ppm in 250N have merged, and the peak at 8.3 ppm in the 250N sample is shifted slightly to higher shielding and increases significantly in relative intensity. This peak continues to shift to higher shielding and increase in intensity with increased temperature, as

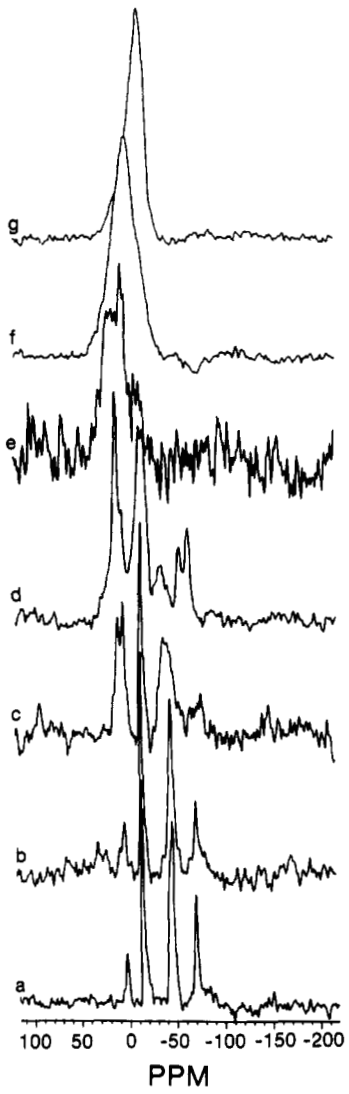

Figure 8. The 29.81-MHz ^{29}Si MAS NMR spectra of isolated VPS samples heated according to schedules in Table I: (a) VPS, (b) 151N, (c) 196N, (d) 250N, (e) 400N, (f) 650N, (g) 1000N.

observed for samples 650N and 1000N. A new, broad peak is seen near 145 ppm in sample 650N and indicates the presence of excess graphitic carbon.[33] This peak sharpens somewhat and shifts to 121 ppm in sample 1000N. The main peak at 19.5 ppm in sample 1000N confirms the formation of SiC.[33-35]

The ^{29}Si solution spectrum of VPS (Figure 5c) exhibits major peaks in four regions, attributed to (1) R_3Si*Si(H)$MeSiR_3$ units (−65 to −80 ppm, broad single main peak);[28] (2) R_3Si*$SiMe_3$ end groups (−10 to −20 ppm, 2 major sharp peaks);[28,32] (3) R_3Si*Si$(Me_2)SiR_3$, R_3Si*Si$(CH{=}CH_2)MeSiR_3$, extended $-(*SiMe_2)_n-$ groups (−40 to −55 ppm, broad multiple peaks);[28] and (4) Me_3*$SiCH_2$Si$(Me_2)SiR_3$ "poly(carbosilane)" units (6 to 0 ppm, broad single main peak). The peak located between 6 and 0 ppm could also arise from extended methylene bridges, $-(CH_2)_n-$, between trimethylsilyl end groups and the polysilane chain, since we attribute this peak to four C atoms surrounding a central Si atom.[28] Although R_3Si–O reso-

(33) Haworth, D. T.; Wilkie, C. A. *J. Inorg. Nucl. Chem.* **1978**, *40*, 1689.

(34) Wagner, G. W.; Na, B.-K.; Vannice, M. A. *J. Phys. Chem.* **1989**, *93*(13), 5061.

(35) Carduner, K. R.; Shinozaki, S. S.; Rokosz, M. J.; Peters, C. R.; Whalen, T. J. *J. Am. Ceram. Soc.* **1990**, *73*(8), 2281.

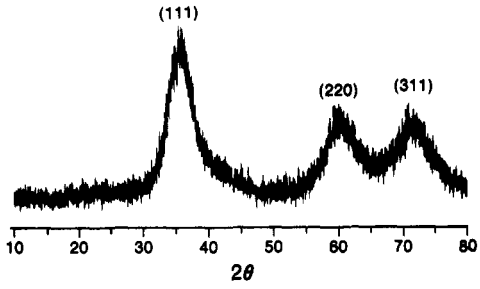

Figure 9. X-ray diffraction powder pattern of sample 1000N, showing partially crystalline β-SiC.

nances would also appear in this region,[14] the low values obtained in the elemental analysis for oxygen (Table IV) makes this alternative assignment unlikely.

The solid-state ^{29}Si spectra of VPS and 151N (Figure 8) show the same features as the solution spectrum of VPS. Solid-state ^{29}Si peak positions for neat VPS are noted in parentheses. With heating to 196 °C, the intensity of the peak assigned to $R_3Si^*Si(H)MeSiR_3$ (−72.1 ppm) decreases, the peak attributed to $R_3Si^*Si(CH{=}CH_2)MeSiR_3$, $R_3Si^*Si(Me_2)SiR_3$, and $-(^*SiMe_2)_n-$ structures (−47.2 ppm) broadens and shifts to lower shielding (−40.6 ppm), and the peak attributed to $R_3{}^*SiCH_2{}^*SiR_3$ (1.3 ppm) linkages increases in intensity and is resolved as two peaks at 7.20 and 1.96 ppm. The peak assigned to the $R_3Si^*SiMe_3$ (−16.3 ppm) functionality remains unchanged.

At 250 °C, two new peaks in the ^{29}Si spectrum of 250N, attributed to a SiH functionality, have increased in relative intensity and shifted to lower shielding (−57.0 and −66.8 ppm). The $R_3Si^*Si(Me_2)SiR_3$ peak has decreased further in intensity and shifted to −38.7 ppm. An intense peak remains at 7.86 ppm for the $R_3{}^*SiCH_2{}^*SiR_3$ unit. The $R_3Si^*SiMe_3$ peak centered at −16.3 ppm has broadened considerably and lost intensity.

The 400N, 650N, and 1000N samples show only one broad peak, indicating that all silicon atoms are situated in chemically similar but not identical environments. This broad peak is typical of "amorphous" or partially crystalline silicon carbide. Upon heating from 400 to 1000 °C, the maximum of this peak shifts to higher shielding from about 13 to −14.3 ppm, which is in good agreement with reported values of −18 ppm for the single peak of β-SiC[35-37] and −14, −20, and −25 ppm for the three peaks observed for α-SiC.[35,36] The peak shift is consistent with increased crystallization of the amorphous preceramic, and the slightly lower shielding than literature values[35-37] is probably caused by incomplete crystallization of the β-SiC.

(e) Crystallinity: X-ray powder diffraction experiments suggest that sample 650N is amorphous while sample 1000N consists of partially crystalline β-SiC, which agrees with previous observations.[7a,12] The diffraction pattern of sample 1000N is seen in Figure 9. Three broad peaks are observed at $2\theta = 36°$, 61°, and 72°, which correspond to the (111), (220), and (311) planes of β-SiC, respectively. The peak widths were used to calculate an average particle size of 2.3 nm, which is in agreement with Bishop's earlier report.[12]

(f) Compositional analysis of VPS: An approximate structural formula of VPS was determined by using solid-state ^{29}Si and solution ^1H NMR spectra. Integration of the ^{29}Si spectra provided relative amounts of each silicon functional group, and ^1H NMR distinguished between Me_2Si and $Me_2SiCH{=}CH_2$ functionalities. The proposed composition

$$[[(SiMe_3)]_{0.32}[Si(CH{=}CH_2)Me]_{0.35}[Si(H)Me]_{0.18}\text{-}[SiMe_2]_{0.07}[CH_2SiMe_3]_{0.08}]_n$$

is in reasonable agreement with the elemental analysis obtained for as-received VPS for Si (calc 41.9%, anal. 44.73%), C (calc 47.5%, anal. 46.31%), and H (calc 10.5%, anal. 8.88%). The polymer contains major fractions of trimethyl- and vinyl-substituted silicon units and a significant portion of hydrido-substituted silicon, which agrees with the structure proposed by Schilling for the sodium-derived polymer.[7a] We also detected a minor fraction of dimethyl-substituted silicon, which may have arisen from the use of dimethyldichlorosilane as a starting materal.[7a] The presence of the minor poly(carbosilane) fraction may be due to methylene insertion induced by heating during the preparation of the polymer.

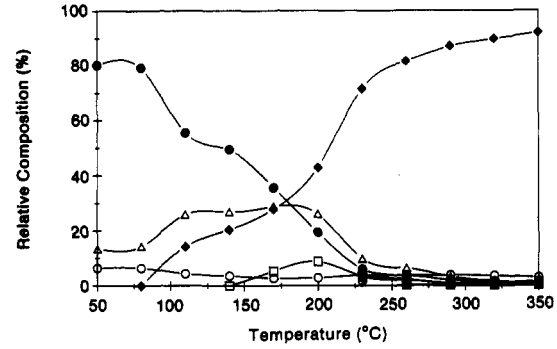

Figure 10. Relative concentrations of gaseous byproducts obtained from the decomposition of VPS in N_2 as a function of temperature; ○, methane; ●, ethane; △, ethylene; ▲, propane; □, propene; ■, isobutane; ▽, *n*-butane; ▼, methylsilane; ◇, dimethylsilane; ◆, trimethylsilane; ◑, tetramethylsilane.

(g) Gas analysis: Decomposition of the polymer in N_2 was examined by analysis of the volatile gases by GC, GC/FTIR, and GC/MS. Figure 10 compares the relative proportions of the major decomposition gases as a function of temperature. Qualitative analyses of the volatile gases were accomplished by GC/MS and GC/FTIR. Quantitative estimates of the relative amounts of the evolved gases were made by integration of GC peaks (TC detector). Below 100 °C, nearly 80% of the detected volatile species evolved is ethane, with smaller fractions of ethylene and methane present. The proportion of ethane evolved relative to other evolved gases decreases with increasing pyrolysis temperature, so that by 250 °C very little ethane is given off. Above 100 °C, trimethylsilane is evolved, increasing in proportion to nearly 40% at 200 °C, and comprising at least 90% of the gases evolved by 350 °C. In the 300–750 °C range, where most of the weight loss of VPS occurs (Figure 1), trimethylsilane continues to be the primary gas evolved, along with increasing, but minor proportions of C_3 and C_4 hydrocarbons and methyl-, dimethyl-, and tetramethylsilane. GC/MS also confirms minor amounts of methylethylsilane and diethylsilane. Although hydrogen probably evolves during both the cross-linking and the decomposition of the polymer, it was not investigated.

(h) ESR analysis: Preliminary ESR experiments revealed that sample 151N contains no detectable spin density (sensitivity limit 1×10^{16} spins/g), but sample 400N contains a free spin density of 2×10^{16} spins/g, which increased to 2.47×10^{19} spins/g in 650N and 1.68×10^{20} spins/g in sample 1000N.

(36) Inkrott, K. E.; Wharry, S. M.; O'Donnell, D. J. *Mater. Res. Soc. Symp. Proc.* **1986**, *73*, 165.
(37) Finlay, G. R.; Hartman, J. S.; Richardson, M. F.; Williams, B. L. *J. Chem. Soc., Chem. Commun.* **1985**, 159.

Discussion

Controlled thermolysis of VPS to 1000 °C in N_2 produces a C-rich SiC ceramic. The polymer-to-ceramic conversion involves at least three main stages: (1) cross-linking and loss of low molecular weight oligomers below 300 °C; (2) polymer degradation, which is characterized by significant decomposition of the side groups and chain scission, along with conversion of the polysilane skeleton to poly(carbosilane), between 300 and 750 °C; (3) crystallization of fine-grain β-SiC above 750 °C, with continued loss of side groups and increased densification of the polymer. Poly(carbosilanes) are known to decompose above 300 °C with loss of side groups and chain scission,[5,9] including transition through an amorphous state prior to crystallization.[5h]

Cross-Linking. VPS contains a significant portion of vinyl groups that increase the char yield of SiC during the conversion of the polymer to ceramic. Unsaturated side groups can increase the yield of SiC derived from polysilanes[17] and retard weight loss during pyrolytic decomposition.[38] The IR data of Figures 2 and 4 show that significant cross-linking of VPS occurs at approximately 140 °C and is nearly complete between 200 and 250 °C. The low-temperature (<300 °C) IR data (Figure 2) suggest that elimination of the pendant vinyl groups occurs at a faster rate than the loss of the silicon-hydrogen group in the VPS network during solidification. The decreasing slope between 160 and 400 °C in Figure 2 can be correlated with the diminishing concentration of available vinyl groups in the polymer. The intensity decrease in the asymmetric $=CH_2$ stretch band and broadening of the $Si—CH=CH_2$ deformation band in the FTIR spectrum of 250N (Figure 4) also monitor the changing vinyl vibrational environments that result from cross-linking.

Cross-linking of the vinyl groups can occur by a mechanism involving free radicals, such as eq 1, where R• =

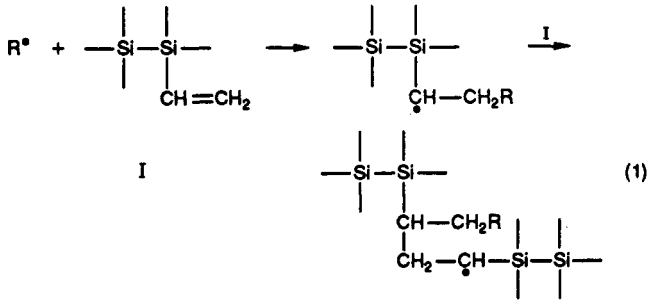

(1)

•CH_3 or •H. This reaction is consistent with our observation that the average molecular weight of VPS is increased by exposure to UV light, as shown in Figure 3. These GPC data also show clearly the effects of the thermally induced cross-linking of VPS, by the increasing proportion of higher molecular weight species as VPS is heated.

There are several potential sources of radical species that would initiate the above cross-linking reaction. Hydrogen and methyl radicals are proposed as radical sources during the decomposition of poly(carbosilanes).[9a] Both species are likely produced by the dissociation of Si–H and $Si–CH_3$ functionalities during thermolysis of VPS, since these groups are abundant in VPS and intermediates isolated at 250 °C and below. The homolytic dissociation of the C–H bond is also reported to occur prior to cleavage of Si–C in free-radical reactions of organosilicon compounds.[5a]

However, the Si–Si bond dissociation energy is considerably lower than that of the Si–C, Si–H, or C–H bonds.[39,40] The scission of the $-(Si–Si)_n-$ chain to produce small concentrations of silyl radicals, $R_3Si•$, is proposed as a major radical source at the low temperatures at which cross-linking of VPS occurs. Yajima[5a] and Fritz[41] proposed similar mechanisms for polysilanes prior to re-formation of a $-(Si–C)_n-$ backbone. The detection of trimethylsilane as the primary decomposition product (Figure 10) supports this mechanism. Trimethylsilane could result from abstraction of a H group by the trimethylsilyl radical. Similarly, abstraction of a CH_3 group could produce tetramethylsilane. Temperatures below 300 °C are lower than those reported previously,[42] where temperatures near 600 °C were needed to homolytically cleave the Si–Si bond of hexamethyldisilane.

In addition to the polymerization of the vinyl groups initiated by radicals, cross-linking reactions that eliminate Si–H groups also occur, as evidenced by the decrease and broadening of the Si–H stretch absorption band in sample 250N, as compared to that in VPS, in Figure 4. These changes could be due to a combination of hydrosilylation (eq 2), H-abstraction (eq 3), or elimination of H_2 with consequent Si–Si bond formation (eq 4). Schilling observed a similar decrease in the Si–H stretch intensity below 300 °C.[7a]

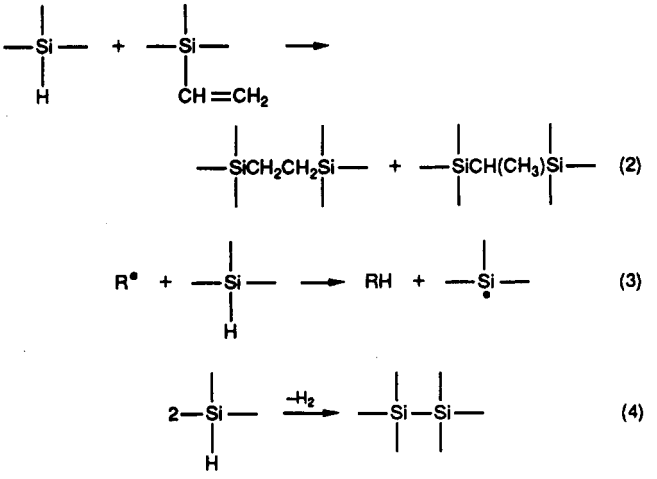

The ^1H, ^{13}C, and ^{29}Si solid-state NMR data at intermediate stages of pyrolysis of VPS corroborate the IR evidence for reactions involving the pendant vinyl groups, the hydrido groups, and Si–Si linkages in the polysilane chain of VPS. The ^1H CRAMPS peak near 6 ppm (Figure 6), associated with the vinyl group, reduces to negligible intensity by heating VPS to 250 °C. The same trend is noted in the ^{13}C MAS NMR spectra of Figure 7, as the vinyl group peak intensity near 138 ppm disappears by 250 °C. This trend is also seen in the ^{29}Si MAS NMR spectra (Figure 8), where the peak originally near −47 ppm, associated with the $SiCH=CH_2$ unit, shifts to lower shielding (ca. −30 ppm) with significantly reduced intensity, by heating at 250 °C.

The ^{29}Si MAS NMR spectra of samples VPS, 151N, 196N, and 250N confirm the loss of Si–H functionality at pyrolysis temperatures below 250 °C, as seen by a decreasing SiH peak at ca. −72 ppm (Figure 8). The si-

(38) Wynne, K. J.; Rice, R. W. *Annu. Rev. Mater. Sci.* **1984**, *14*, 297.

(39) Walsh, R. *Acc. Chem. Res.* **1981**, *14*, 246 and references therein.

(40) Cottrell, T. *The Strength of Chemical Bonds*, 2nd ed.; Butterworths: London, 1958.

(41) Fritz, G.; Grobe, J.; Kummer, D. *Adv. Inorg. Chem. Radiochem.* **1965**, *7*, 349.

(42) Shini, K.; Kumada, M. *J. Org. Chem.* **1958**, *23*, 139.

multaneous appearance of new methylene resonances in the ^{13}C MAS NMR spectra (Figure 7) supports the hydrosilylation mechanism (eq 2).

The strong $SiCH_2Si$ deformation (1046 cm^{-1}) in the IR spectrum of as-received VPS (Figure 4) and the ^{29}Si MAS NMR peak at 1.3 ppm (Figure 8) show that the VPS precursor consists primarily of a Si–Si backbone chain with a small polycarbosilane component. The presence of a small amount of SiOSi polysiloxane cannot be excluded on the basis of IR and NMR observations, although the relatively low value for percent O obtained by elemental analysis (Table IV) suggests that the proportion of these groups in the as-received polymer is small. The band at 1046 cm^{-1} has also been assigned to the SiOSi stretching vibration.[24] This vibration has a very large molar absorptivity, such that the presence of less than 1% of oxygen can be detected by IR. It is possible that a small concentration of SiOSi linkages was incorporated into the polymer during synthesis or that the polycarbosilane portion has reacted with trace moisture.[24] The decreased intensity of the Si–H stretch on heating to 250 °C and the subsequent increased intensity of this band after heating to 400 °C are consistent with earlier reports that confirmed that hydrosilylation occurs during the decomposition of polycarbosilane.[7a] The decrease and then increase in the concentration of the Si–H functionality are also consistent with the ^1H CRAMPS spectra of sample 400N and the ^{29}Si NMR data. Cross-linking through vinyl groups and hydrosilylation mechanisms give rise to at least two chemically distinct methylene environments, which were observed experimentally as distinct resonances in the ^{13}C MAS spectra (Figure 7).

Polymer Degradation. The decomposition chemistry of VPS above 300 °C is quite complex and involves restructuring of the polymer backbone as well as substantial cleavage of the side groups.

The intensities of the Si–H stretching band and the $Si–CH_2–Si$ deformation band increased with an increase in pyrolysis temperature from 250 to 400 °C (Figure 4) as a result of methylene insertion (eq 5). This mechanism

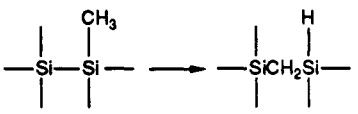

(5)

is the basis for Yajima's conversion of poly(dimethylsilanes) to poly(carbosilanes).[5f] Methylene insertion reactions are also suggested by changes in the ^1H CRAMPS, ^{13}C MAS, and ^{29}Si MAS NMR spectra. The observation of more than one distinct methylene carbon/proton resonance is consistent with the complicated chemistry of the system, wherein different reactions generate chemically distinct methylene environments.

Following the conversion of VPS to "poly(carbosilane)" at higher temperatures (300–750 °C), the Si–H functionality is likely to be the major radical source, since it has the lowest bond energy in the poly(carbosilane) skeleton.[43]

Silylenes, R_2Si:, are another likely radical source and have been proposed as the main reaction intermediates during the gas-phase pyrolysis of methylsilanes;[39,44-47] there is also evidence for the trapping of dimethylsilyene by butadiene.[46] Silylenes can insert into a Si–H bond to extend the silane chain and quench the radical. Combinations of radical- and silylene-producing reactions are also postulated to occur in a variety of silane reactions.[48-50] Preliminary ESR experiments indicate that a substantial concentration of free radicals is present in the isolated solid samples 400N, 650N, and 1000N, which corroborates the participation of radical species during the decomposition of VPS.

Assuming the production of proton, methyl, or trimethylsilyl radicals or silylene diradicals, one would anticipate the eventual production and evolution of gaseous products such as ethane, ethylene,[50] propane, propene, and substituted silanes on pyrolysis of VPS. All of these species were observed by GC/MS and GC/FTIR, as seen in Figure 10. The methane could arise from abstraction of hydrogen by methyl radicals or as a byproduct from a silylene reaction. The primary source of methyl radicals is probably the methyl groups attached to the silicon backbone of the precursor.

A variety of radical combination and abstraction reactions are possible at high temperature and can account for the various hydrocarbon and silane products observed. No attempt was made in this work to quantify the source of these volatilized species from structural components of VPS.

^1H CRAMPS spectra of the partially pyrolyzed VPS samples confirm the decreasing concentration of hydrogen with increasing pyrolysis temperature. The ^{13}C MAS NMR spectra demonstrate the coalescence of the various $Si_w–C_y$ units to a single peak representing SiC_4 units in SiC and incorporation of excess carbon into the resulting ceramic product. ^{29}Si MAS NMR spectra show the conversion of four chemically distinct Si environments to one of preceramic SiC.

Crystallization of VPS to β-SiC. Following the major weight loss of VPS upon pyrolysis, considerable excess carbon is present in the sample, as measured by the Si/C ratio from elemental analyses and ^{13}C solid-state NMR spectroscopy. In contrast to the partially crystalline β-SiC, the excess carbon in 1000N was not observed by X-ray diffraction, due to its amorphous character and perhaps due to its lower scattering efficiency than that of SiC.[12] $^1H \rightarrow {}^{13}C$ cross polarization NMR experiments indicate that even after heating to 1000 °C, there remains a significant hydrogen concentration in the ceramic, which may act to increase bonding saturation around C and Si centers. ESR spectra of the 1000N sample also suggest a large concentration of free radicals which are likely to be associated with incompletely bonded C or Si sites. Heating to 1900 °C is required to fully crystallize VPS-derived SiC and increase the crystallinity of the excess carbon,[12] presumably with loss of excess H and radical coupling. The shifts and sharpening of the ^{13}C and ^{29}Si MAS NMR peaks as well as the IR spectrum of sample 1000N confirm the increased crystallinity of ceramic β-SiC.

Conclusions

Solid-state NMR, in conjunction with other analytical techniques such as IR, thermal analysis, and XRD, provided elucidation of the various structural changes that occur during the pyrolysis of VPS. These changes include

(43) Taki, T.; Inui, M.; Okamura, K.; Sato, M. *J. Mater. Sci. Lett.* **1989**, *8*, 918.
(44) Atwell, H. W.; Weyenberg, D. R. *Angew. Chem., Int. Ed. Engl.* **1969**, *8*, 469.
(45) O'Neal, H. E.; Ring, M. A. *Organometallics* **1988**, *7*, 1017.
(46) Clarke, M. P.; Davidson, I. M. T.; Dillon, M. P. *J. Chem. Soc., Chem. Commun.* **1988**, 1251.
(47) Davidson, I. M. T.; Ring, M. A. *J. Chem. Soc., Faraday Trans. 1* **1980**, *76*, 1520.
(48) Neudorfl, P. S.; Strausz, O. P. *J. Phys. Chem.* **1978**, *82*, 241.
(49) Gusel'nikov, L. E.; Polyakov, Y. P.; Volnina, E. A.; Nametkin, N. S. *J. Organomet. Chem.* **1985**, *292*, 189.
(50) Ring, M. A.; O'Neal, H. E.; Rickborn, S. F.; Sawrey, B. A. *Organometallics* **1983**, *2*, 891.

cross-linking by vinyl polymerization with some hydrosilylation at low temperatures, extensive Si-Si, C-H, and Si-H bond cleavage with radical formation and methylene insertion at intermediate temperatures, and finally consolidation of the "SiC" network, along with the formation of free carbon and partial crystallization of the ceramic product at higher temperatures. ^{1}H, ^{13}C, and ^{29}Si MAS NMR reveal structural details of the polymer-to-ceramic conversion that are unavailable by typical XRD techniques and give insight into the chemical bonding and phase composition of these inorganic amorphous polymers.

The application of solid-state NMR, along with other analytical methods, has provided an improved understanding of the chemical decomposition of a commonly used vinylic polysilane precursor to ceramic SiC. This information should assist in designing new ceramic precursors to meet specific processing objectives, such as the enhancement of ceramic yield and the production of innocuous byproducts, or with tailorable physical properties, such as solubility and viscosity, for preparation of thin films or continuous fiber.

Acknowledgment. We acknowledge the support of the National Science Foundation under Materials Chemistry Initiative Grant No. CHE-8706131 and the Colorado State University Regional NMR Center, funded by NSF Grant No. CHE-8616437. C. E. Bronnimann provided invaluable assistance in obtaining CRAMPS spectra. W.R.S. acknowledges Dr. G. M. Renlund at General Electric Corporate Research and Development for assistance with TGA/DTA experiments, Mr. W. Hurley, Jr., for assistance with isolation of preceramic materials and determination of the proposed composition of the vinylic polysilane, Mr. C. Warren for preliminary analyses of decomposition gases, and Mr. C. Whitmarsh for insightful NMR discussions. Dr. C. L. Czekaj is thanked for solution NMR experiments. Mr. R. Lewis is acknowledged for ESR experimental work.

Registry No. SiC, 409-21-2.

Loss of Halide from Sol-Gel Films on Heating Does Not Involve Oxidation[1]

Carol L. Schutte[†,‡] and George M. Whitesides*[,†]

Department of Chemistry, Harvard University, Cambridge, Massachusetts 02138, and Department of Materials Science and Engineering, Massachusetts Institute of Technology, Cambridge, Massachusetts 02139

Received July 11, 1990. Revised Manuscript Received December 5, 1990

The loss of halide ion from sol-gel-derived films on heating has been studied by Rutherford backscattering spectrometry. The rates of loss of halide under air and argon atmospheres were very similar. This observation is consistent with a nonoxidative mechanism for the loss of halide. The relative rate of loss of halide at a particular temperature follows the qualitative order LiI > LiBr ≃ LiCl > NaI > NaBr > KI ≃ KBr ≃ NaCl. This order correlates with the vapor pressures of the salts and with the ΔG of formation of the hydrogen halides by reaction of metal halide with water and suggests that volatilization of the salt and/or the hydrogen halide is the mechanism for loss of halide ion from sol-gel coatings.

Introduction

Hydrogen halides and halide salts are catalysts used in sol-gel reactions to affect the time required for gelation.[2,3] Chlorine gas dehydroxylates surface silanols in sol-gel-derived glass during sintering. This reduction in OH content avoids bubbling or foaming of the glass on further heating.[4] Little is known about the fate of the ions after gelation or sintering, although the halides are known to disappear from the gel during its transformation to glass at high temperatures. The goal of this study was to investigate the mechanism of loss of halide ion from sol-gel coatings on heating. We have used Rutherford backscattering spectrometry (RBS) to quantify the content of halide ion (and non-halogen anions) in silica films derived from sol-gels as a function of the temperature and atmospheres under which they were heated. We have also used Auger electron spectroscopy (AES) for qualitative analysis for the presence of sodium in a NaI-doped SiO_2 sample both before and after thermal treatment.

Mechanisms for the Loss of Halide in Sol-Gel Coatings. Halogen could, in principle, be lost from the silica film either as HX or M^+X^- or, following oxidation, as X_2 (eqs 1-4; Si_l denotes a representative silicon center volatilization of HX:

$$Na^+X^- + HOSi \rightarrow HX\uparrow + NaOSi_l \quad (1)$$

$$Na^+X^- + HOH \rightarrow HX\uparrow + NaOH \text{ (or } Na_2O) \quad (2)$$

volatilization of MX:

$$Na^+X^- \rightarrow Na^+X^-\uparrow \quad (3)$$

oxidation of X^- to X_2:

$$2Na^+X^- + \tfrac{1}{2}O_2 \rightarrow X_2\uparrow + Na_2O \quad (4)$$

in the silicate lattice). It is possible that mass transport of some species (M^+X^-, HX, X^-, X_2, O_2, H_2O) might be rate-limiting. The only plausible oxidant under normal

[†] Harvard University.
[‡] Massachusetts Institute of Technology.

(1) Supported in part by the National Science Foundation (CHE-88-12709), the Office of Naval Research, and the Defense Advanced Research Projects Agency (through the University Research Initiative). The Cambridge Accelerator for Materials Science was purchased through a DARPA/URI grant and is housed in the Harvard University Materials Research Laboratory, an NSF-funded facility (DMR-86-14003).

(2) Pope, E. J. A.; Mackenzie, J. D. *J. Non-Cryst. Solids* **1986**, *87*, 185-198.

(3) Melpolder, S. M.; Coltrain, B. K.; Salva, J. M. In *Proceedings of the Fourth International Conferences on Ultrastructure Processing of Ceramics, Glasses, and Composites, Tucson, Arizona, February, 1989*; Uhlmann, D. R., Ulrich, D., Eds., to be published.

(4) Shin Satoh, I.; et al. U.S. Patent 4,426,216, Jan 1984.

0897-4756/91/2803-0267$02.50/0